

Engine integration of high aspect ratio rectangular jet nozzle (unheated subsonic flow)

Christian Jente*

German Aerospace Center (DLR), Lilienthalplatz 7, D-38108 Braunschweig, Germany

Jet noise is a crucial component in the entire mix of aircraft-relevant noise sources. A quiet aircraft requires a low noise engine integration. Compared to the conventional round jet engine, the jet potential core length is shorter for a rectangular jet engine with same nozzle outlet area. This is especially true for high aspect ratio rectangular jets (here AR 13.3). Hence, the engine integration of the rectangular nozzle onto a wing could be conducted in a way where jet noise is shielded from an observer at the ground. Yet, the question is how such a low noise engine integration should be designed.

Therefore, an experimental setup was built at the Aeroacoustic Wind tunnel Braunschweig (AWB) where rather large engine integration lengths and heights between engine lip and plate trailing edge can be studied. This allows to test shielding effects of embedded engine systems, e.g. short and long aft-decks, backward-facing steps as well as non-embedded/poled engines.

The contributions of this paper are made in terms of the aero-geometric characterization of the problem physics, the evaluation of the installation effect for observers on the ground (along flyover arc or overhead position) as well as the evaluation of the shielding effect.

The aero-geometric analysis helps to predict acoustical effects which occur for three general installation problems: the asymmetric nozzle, jet-surface interaction as well as wide-angle installations.

Shielding benefits due to the installation of a plate can be determined by a shielding frequency criterion. Unfortunately, the high-frequent noise reduction comes with a low-frequent installation penalty, thereby making noise reduction a difficult design mission: All in all, only one tested configuration shows an overall installation noise benefit.

The general results of rather achieving design penalties for long bevel/aft-deck design and step configurations is in agreement with previous studies conducted by NASA and Georgia Tech. Future low noise rectangular engine integrations may therefore consist of rather small engine integration lengths.

I. Motivation

This paper studies subsonic rectangular jets with high aspect ratios. These nozzle types are mostly known from military aircraft configurations. Furthermore, spatial needs of close engine integration (to fit to the wing) drive the development of more rectangularized nozzle configurations, e.g. oval engines. These developments provide good reason to study the subsonic behavior of rectangular jets and their use in certain installation situations.

*Research Engineer, Department of Technical Acoustics, christian.jente@dlr.de

Abbreviations

AR	aspect ratio, here defined as nozzle height to nozzle width
AWB	Aeroacoustic Windtunnel Braunschweig
DLR	Deutsches Zentrum für Luft- und Raumfahrt e.V., i.e. the German Aerospace Center
ENG	centerpoint of engine (bypass) nozzle outlet, a measurement reference point
NASA	National Aeronautics and Space Administration
S/L	shear layer
w/o	without

Nomenclature

Δf	[Hz]	narrowband frequency bandwidth
ΔU	[m/s]	difference velocity in shear layer
ϕ_{geo}	[°]	geometric build angle
θ	[°]	polar angle, front-aft
a_∞	[m/s]	speed of sound
A_j	[m ²]	cross-sectional area of jet
D_{eq}	[m]	equivalent diameter (same jet area)
f	[Hz]	frequency
$f_{1/3}$	[Hz]	third-octave mid-band frequency
f_{sc}	[Hz]	scaling frequency
f_S	[Hz]	shielding frequency (over vs. under)
H	[m]	step height / plate distance
H_0, h	[m]	characteristical duct height
He	[-]	Helmholtz number
L	[m]	plate integration length
L_{pot}	[m]	jet potential core length
M, M_j	[-]	(jet) Mach number
$OASPL$	[dB]	overall sound pressure level
R	[m]	microphone distance
r_U	[-]	velocity ratio between flight and jet speed
SPL	[dB]	sound pressure level
SPL_{nb}	[dB]	narrowband sound pressure level
Str	[-]	Strouhal number
U	[m/s]	streamwise velocity
U_∞	[m/s]	flight velocity
U_j	[m/s]	jet velocity

II. The model: High aspect ratio nozzles and installation devices

The aspect ratio (AR) of a nozzle is the ratio of nozzle width to nozzle length. High aspect ratio rectangular nozzles can have noise benefits in the rearward arc (where the peak noise is located) when compared to round nozzles (see study of Bridges¹).

The potential core length is shorter for a rectangular nozzle of same thrust:

$$L_{pot,rect} \approx 8 \dots 12 \cdot H_0 = 8 \dots 12 \cdot 20 \text{ mm} = 160 \dots 240 \text{ mm} \quad (1)$$

$$D_{eq} = 2\sqrt{20 \text{ mm} \cdot 266 \text{ mm}/\pi} \approx 82 \text{ mm} \quad (2)$$

$$L_{pot,round} \approx 5 \dots 7 \cdot D_{eq} = 412 \dots 576 \text{ mm} \quad (3)$$

Hence, it should be easier to try and shield a rectangular jet rather than a round jet. Installations to the nozzle exit come in two (academical) shapes: the aft-deck and the bevel (see figure 1). Both of the configurations follow the design idea of creating an asymmetrical nozzle exit and are jet noise reduction technologies. Yet, some embedded propulsion systems were rather designed to aerodynamically fit smooth contour lines. This illustrates that the boundary between engine trailing edge treatment and conventional installation/integration device is not really fixed.

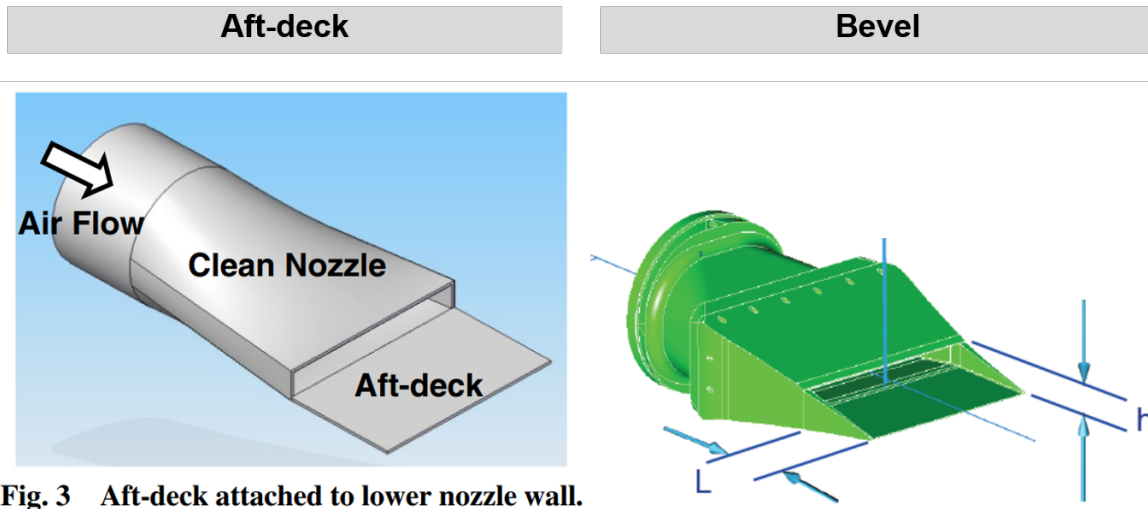


Fig. 3 Aft-deck attached to lower nozzle wall.

Image: NASA, J Bridges, NASA 2012: Acoustic Measurements of Rectangular Nozzles with Bevel

Figure 1: Aft-deck (Behrouzi & McGuirk²) and Bevel configuration (Bridges¹)

One of such studies was performed on the bevel and is available from NASA.¹ Beveled nozzles with a length of $L = 1.4H_0$ and $2.8H_0$ were studied. The configurations look like their design were purposely adapted to neatly fit into the aerodynamic contours near the trailing edge of a wing. A shorter bevel ($L < 1.4H_0$) would probably fit more to the original noise reduction design, yet fits less to an embedded propulsion system).

The academic contribution of this paper is made within the less studied field of aft-deck and backwards facing step configurations where the engine integration lengths L and step heights H are very large. The aft-deck is therefore realized by using a plate whose trailing edge is positioned at various lengths ($L=60, 120, 240\text{mm}$) and heights ($H=0, 10, 20, 100\text{mm}$) downstream the high aspect ratio AR13.3 engine lip ($20\text{mm} \times 266\text{mm}$, see figure 2). The backwards facing step problem is created by implementing a wooden filler. The removal of the filler allows to test the setup of non-embedded engines. A source localization array is placed above plate (door side of windtunnel, see figure 3). It does also include a Brüel & Kjær 4135 microphone (-90°). 8 far-field microphones are positioned below plate at the front-to-aft polar angles of $60^\circ, 75^\circ, 90^\circ, 100^\circ, 110^\circ, 120^\circ, 130^\circ$ and 140° .

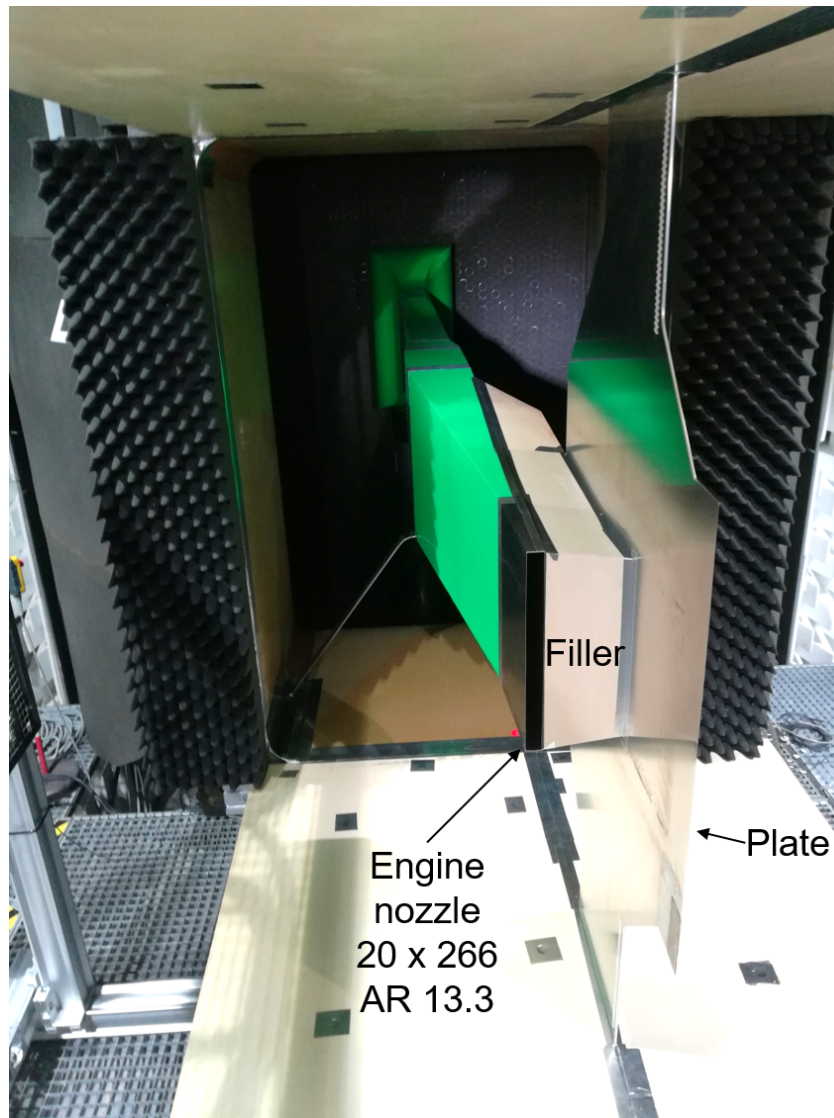


Figure 2: Aero-geometric characterization of the problem physics

III. Test matrix and general test results

A comparison can be made between the case where the plate is installed and where it is not (isolated engine). The tests are mainly conducted for the matrix (figure 4) of $L=[60, 120] \times H=[0, 10, 20]$ and the additional far located setting of $L=100$ and $H=240$ (which is meant to test any potential core shielding benefits). The test results (see figure 5) were evaluated by scaling the measured third-band-octave spectra to full-scale (model scale 1:8), C-weighting the full-scale spectrum and energetically summing up the levels for the Overall Sound pressure level (OASPL).

The tested backward steps and aft-decks (both red) do not help to decrease the noise of the isolated rectangular engine (black). There is a design penalty if such an installation is necessary. The L240 H100 setting is a special case. The statically operated installed noise is of same order as the isolated noise (magenta), but this is not the case for flight operations anymore. The reason behind this is explained in the following sections of detailed analysis. The blue line, a different physical problem type, will also be presented below; this case shows that shielding benefits of a non-embedded over-wing installation were measured and can be exploited in future designs.

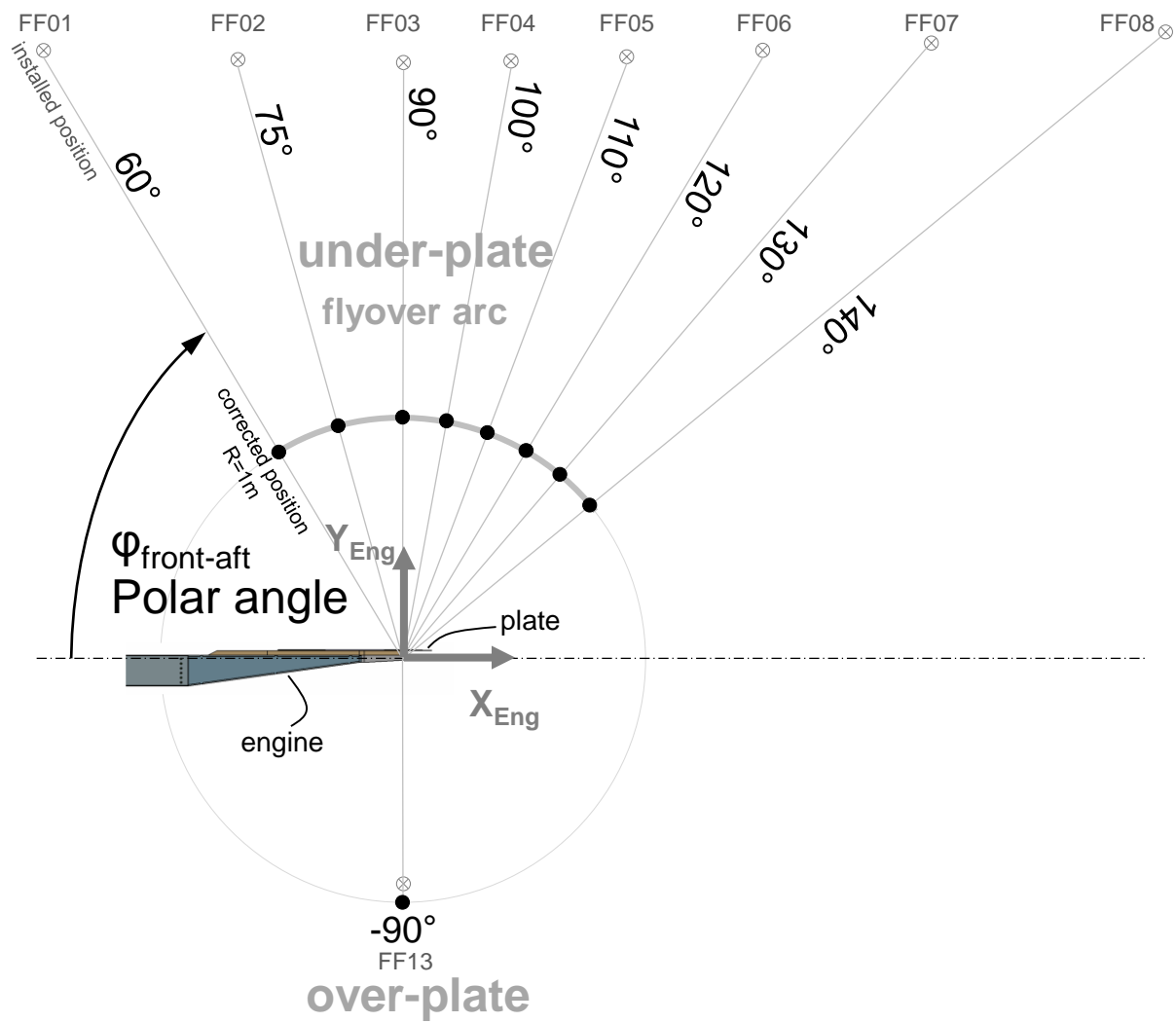


Figure 3: Microphone setup with source localization array and far-field microphones.

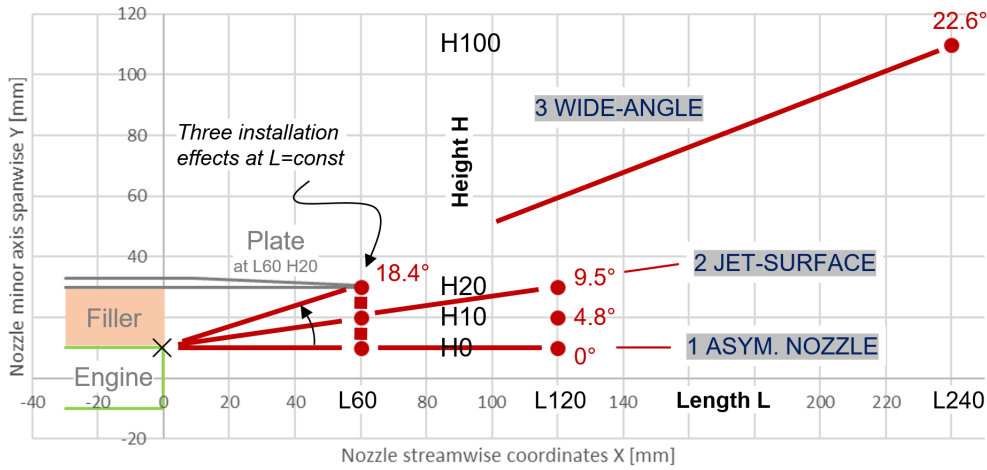


Figure 4: Test matrix with aft-decks and backwards facing step configurations.

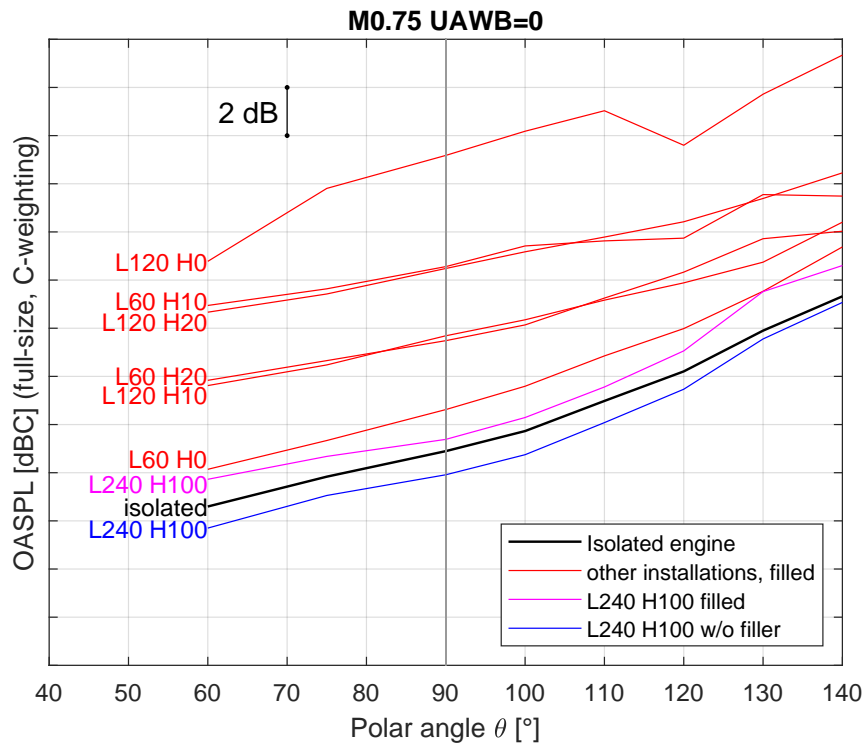
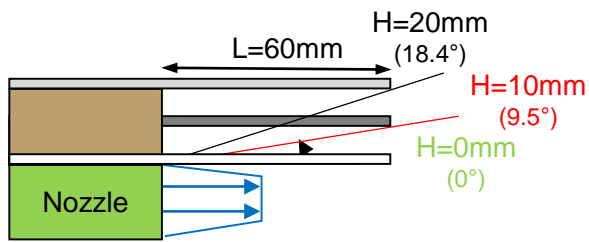


Figure 5: INTONE 1100 test results

IV. The three physical problems on aft-deck and step installations

With the help of plate length $L=60\text{mm}$ and varying height H , three different physical effects can be shown (figure 6), the asymmetric nozzle ($H=0$, green), the jet-surface interaction problem ($H=10$, red) as well as the wide-angle installation ($H=20$, black). All of these settings produce higher SPL than the isolated engine, whereby the jet-surface interaction problem ($H=10$, red) causes particularly high installation noise which includes 4-6 tonal peaks. The source localization maps (displayed in figure 6, bottom right) help to graph the different acoustic effects. The isolated jet is characterized by its low-frequent peak downstream the nozzle (and additional high-frequent noise sources near the engine trailing edge, not shown here). The asymmetric nozzle contains the same high-frequent peaks, but at 4kHz, the additional influence of the plate can be seen. For the jet-surface problem, the noise peaks are located on the plate trailing edge. This is also somewhat true for the wide-angle installation, however the influence of the low-frequent jet peak is also visible. In the following subsections, the three problems shall be briefly studied.



Const. Aft-deck length builds: $L=60\text{mm}$

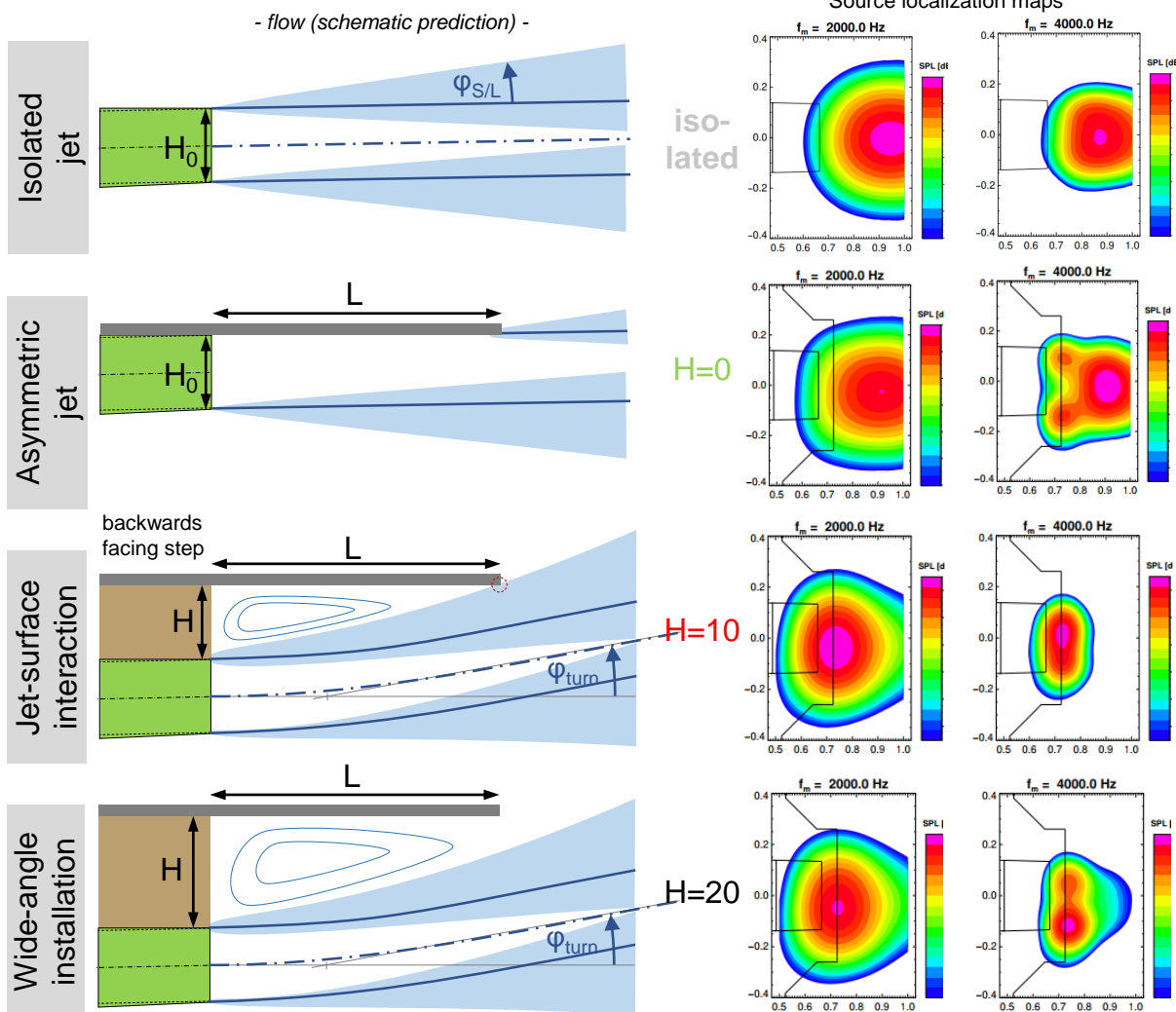
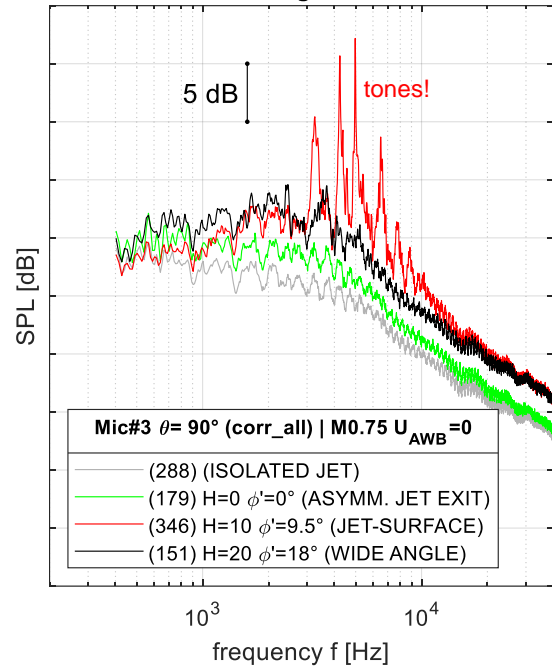


Figure 6: Isolated engine and three general plate installation effects

IV.A. Asymmetric nozzle

The asymmetric nozzle ($H=0$) was studied in two configurations, short (L60) and long (L120) aft-deck (see figure 7). The L120 nozzle (figure 8 left) is prone to tones (up to 25dB, highest OASPL w/o treated plate trailing edge). A static jet study on the problem shows that the tone frequency does not depend on jet Mach number. Tones are not visible in the spectrum until $M=0.58$, but appear at $M=0.64$ (2.4kHz) and $M=0.7$ (4.8kHz). By manipulation of the plate trailing edge (figure 8, right) the presence of the tones can be reduced: The application of serrations slightly prolongs the length and causes the remanence of the tones to show up at lower frequencies ($f \propto 1/L$). Moreover, the broadband noise is diminished by 2-3dB.

If a long aft-deck is to be designed, noise reduction technology on the trailing edge makes a big acoustic difference.

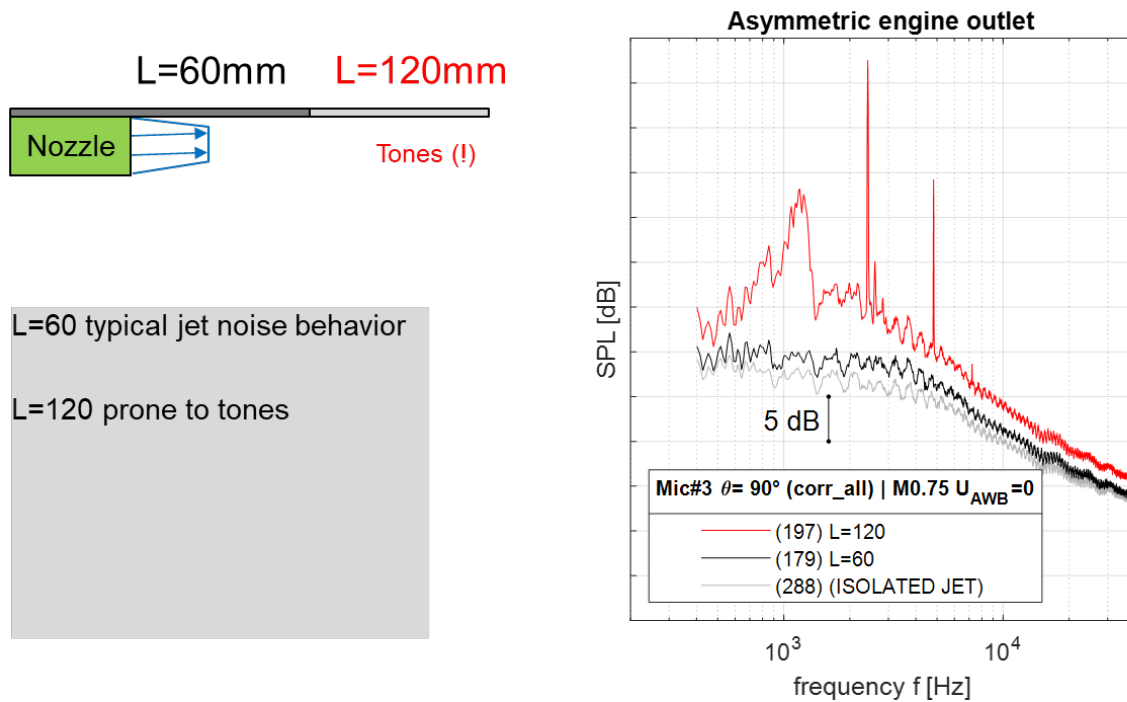


Figure 7: Asymmetric engines with short and long aft-deck.

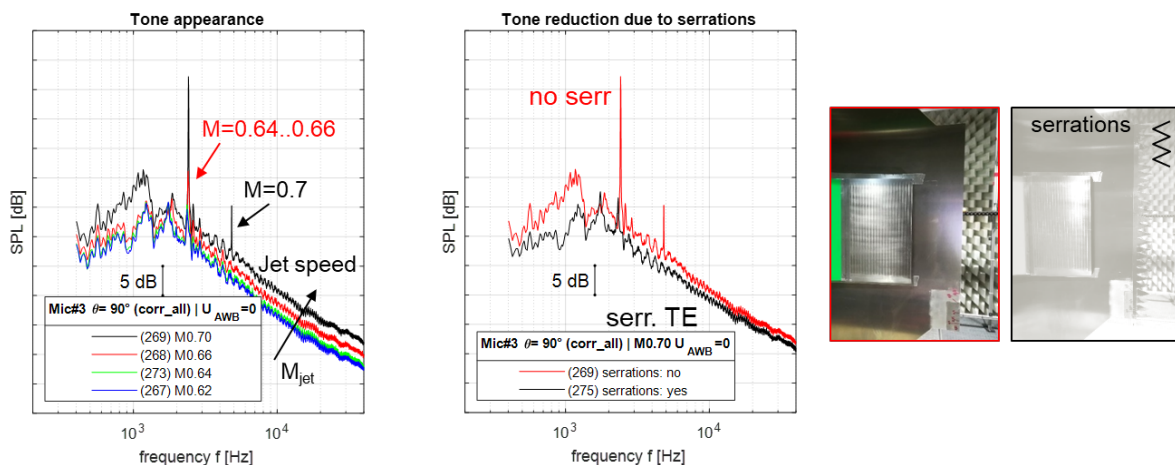


Figure 8: Tone study on long aft-deck (H0 L120)

IV.B. Jet-Surface-Interaction

Jet-plate interaction occurs at certain builds, e.g. the configurations of H10 L60 and H20 L120 which have the same height-length-ratio (1:6), which amounts to 9.5° build angle. Jet-plate interaction is characterized by high SPL including 4-6 tonal components in the spectrum (figure 9). The tones on the long plate correspond to low frequency, whereas the tones on the short plate correspond to high frequencies ($f \propto 1/L$). The frequencies can be normed wrt. the plate length. (The SPL is not scaled,

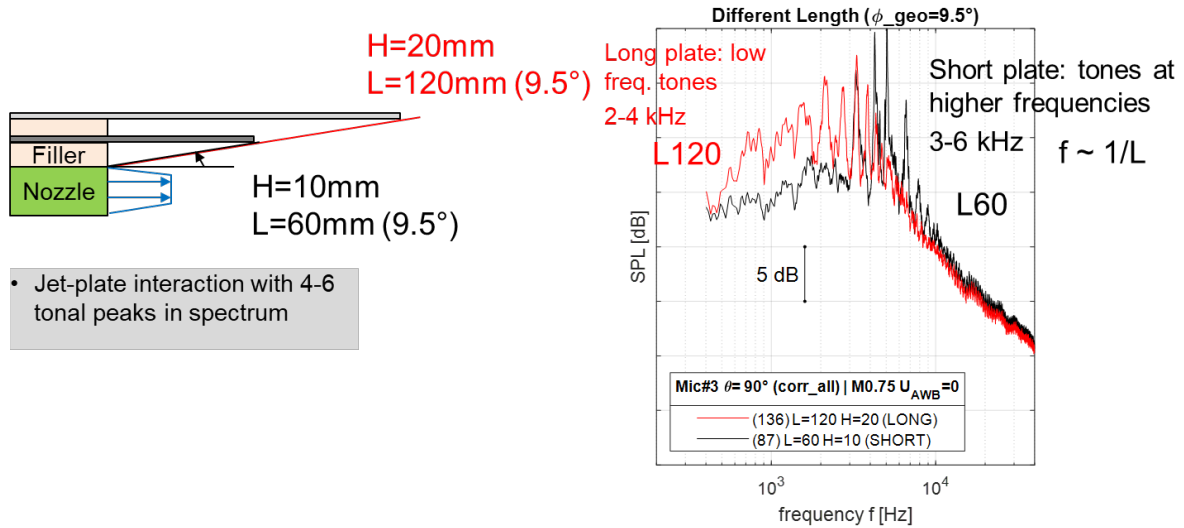


Figure 9: Jet-plate interaction tone frequencies scale with plate length

the idea here is to show the overlapping of frequencies.) The change of the wind tunnel velocity U_∞ parameter causes no significant effect to the spectrum (figure 10 left). The broadband peak depends on plate length L and possibly slightly on jet speed (figure 10 right). The frequency however may potentially follow a Helmholtz analogy ($He = La_\infty/f$).

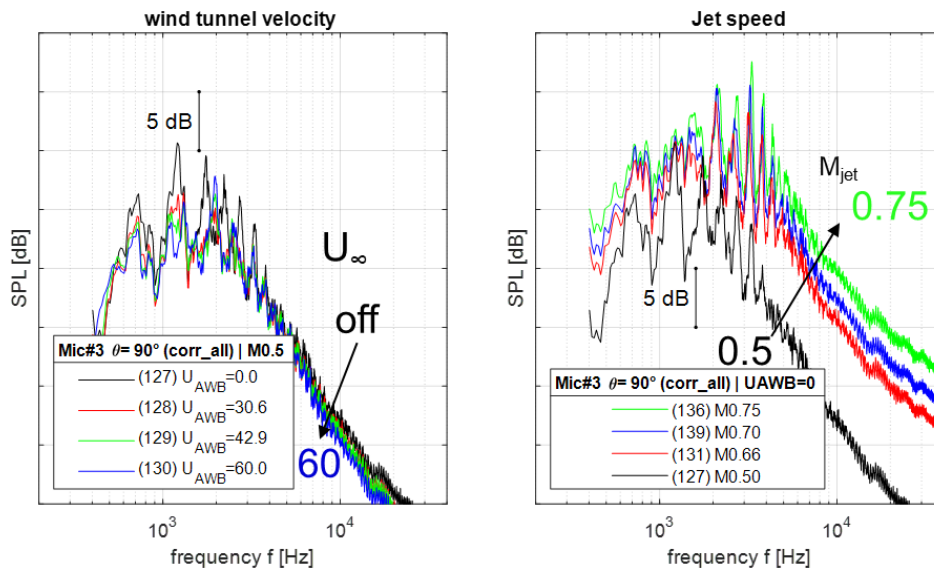
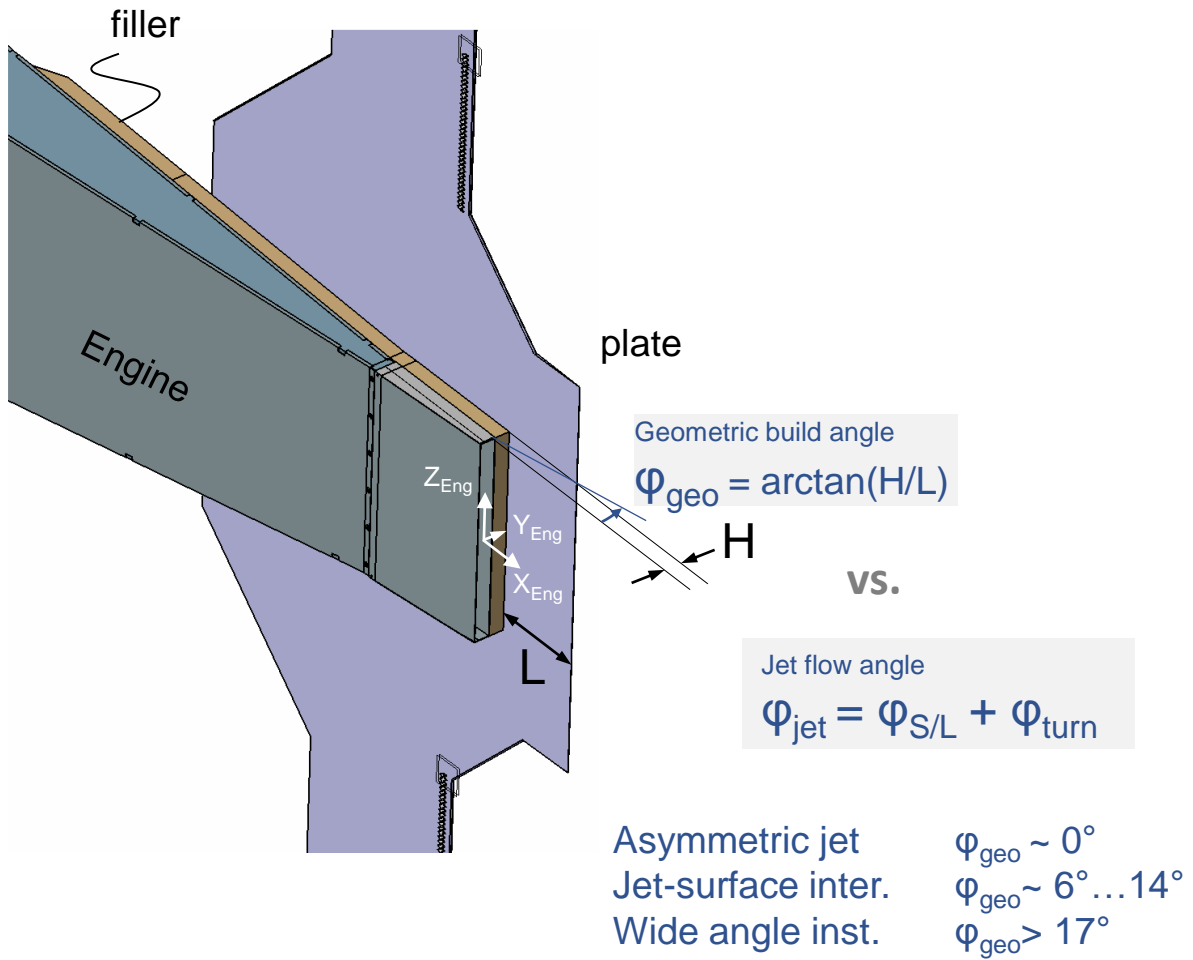
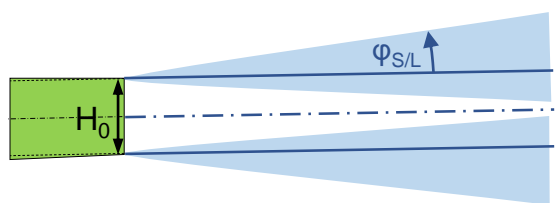


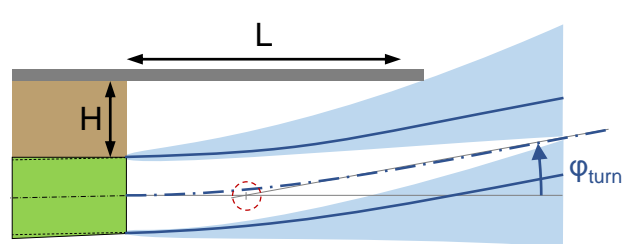
Figure 10: Jet-plate interaction tone frequencies are rather unaffected by jet speed



Half-jet opening angle (isolated)



Flow turning angle (installed)



Steady aerodynamics measurement static jet

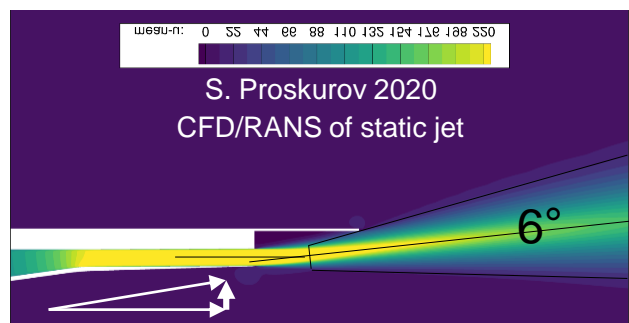
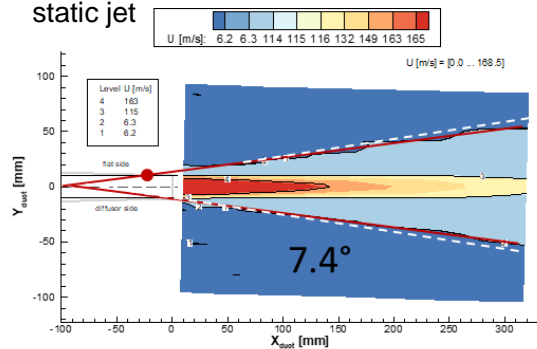


Figure 11: Aero-geometric flow characterization: build space vs. required jet flow space.

ATTEMPT OF AN AERO-GEOMETRIC CHARACTERIZATION A build angle of 9.5° seems to be surprisingly large for expected jet interaction tones, since the half-jet opening angle is typically in the range of 7° - 8° (for static jet; lower angle for flight jet). However, on top of this, jet turning must be accounted for. A RANS simulation for a quasi-static jet shows how the jet turns by 6° from the engine axis (around mid-plate position in figure 11). A rough estimation of the three angles would assume jet-plate interaction in the angular range of 6° to 14° and a wide angle installation above 17° .

The turning of the jet needs be characterized wrt. deflection angle and deflection point for various builds and engine operations in order to complete an aero-geometric model. Such an endeavor is potential aerodynamic future work. Nevertheless, the following hypothesis can be made already:

- In terms of test definition and mounting in the facility, the build parameters of engine integration length L and height H are well-suited. Wrt. the physics of the problem, it is better on the first glance to switch to engine integration length L and build angle ϕ_{geo} : The engine integration length helps with the identification of tones, while the comparison of build angle to flow angle (half-jet opening angle + turning) can help to roughly qualify the general installation type.
- While test operations are defined by jet Mach number M and wind tunnel speed U_∞ , the physics of conventional jet-flap interaction is better characterized by velocity ratio r_U and thrust. The turning which occurs in the backwards facing step problem depends on wind tunnel flow and direction (i.e. influenced by the external engine geometry and the cavity which the step creates). Hence, it seems good to stick with wind tunnel speed and jet Mach number until better flow properties are proposed.

IV.C. Wide angle installations

A rough estimation (figure 11) assumes wide angle installations to occur around 17° and higher. There are two sets which can be evaluated, L60 H20 (18.4°) and L240 H100 (22.6°). Both settings show behavior which is inverse to isolated jet S/L noise (figure 12). Isolated jet shear layer noise is driven by the difference velocity in the shear layer $\Delta U = U_{jet} - U_\infty$. Increasing wind tunnel speed (at same jet speed) causes lower difference velocity and hence lower SPL. The wide-angle installation noise behaves contrary to the isolated jet noise: higher wind tunnel speed causes higher noise. The reason behind this effect may be that higher wind tunnel speed induces higher jet-deflection and therefore stronger interaction with the plate. The L240 H100 step configuration shows a noise benefit for static operations,

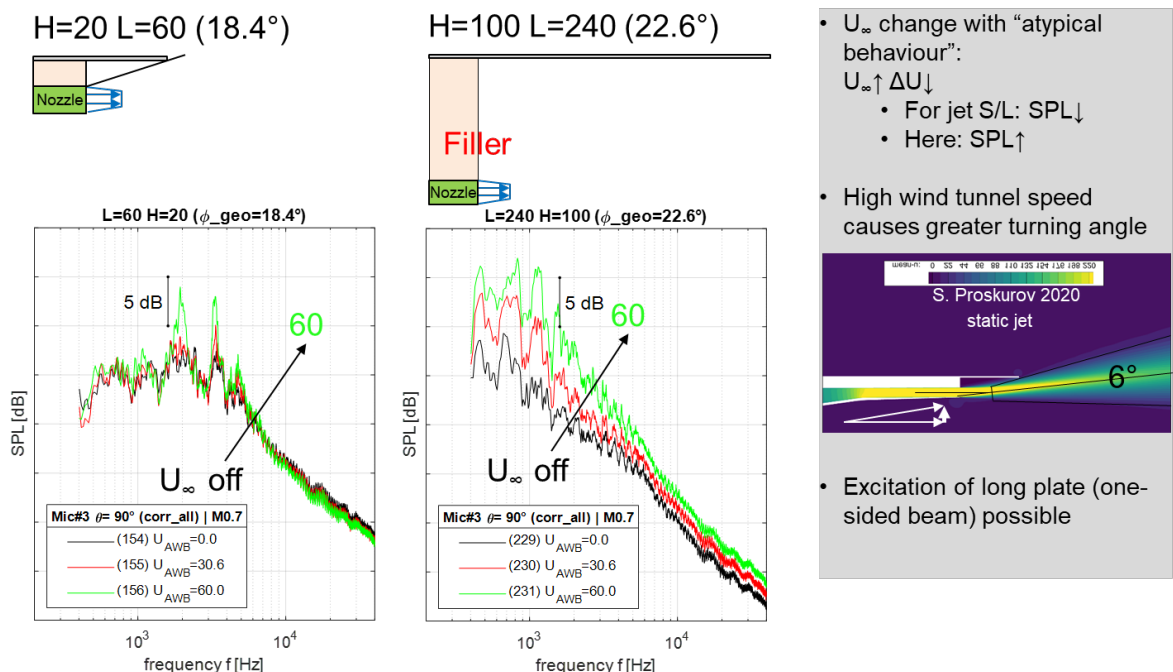


Figure 12: Wide-Angle installations

but not for flight operations. The isolated jet noise (black) decreases with increasing wind tunnel velocity (figure 13, from left to right), but the installation noise (red) increases.

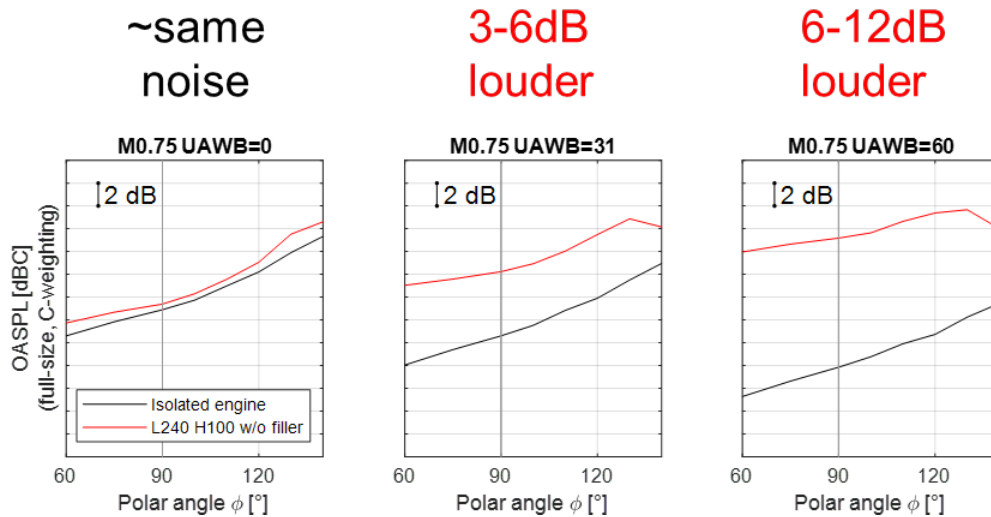


Figure 13: L240 H100 step configuration (w/filler) for static and flight operations

V. Installation effect of non-embedded engines (without filler)

The same L240 H100 configuration can be measured without a filler. There is no connection between the nozzle and the plate. The installation noise decreases in the same fashion as isolated noise (figure 14, left). Shielding benefits are in the region of 0-1dB and prominent in the rear-ward arc (figure 14, right). This shows that conventional shielding works. A possible installation would be a non-embedded propulsion system, i.e. an over-wing installation with a pylon.

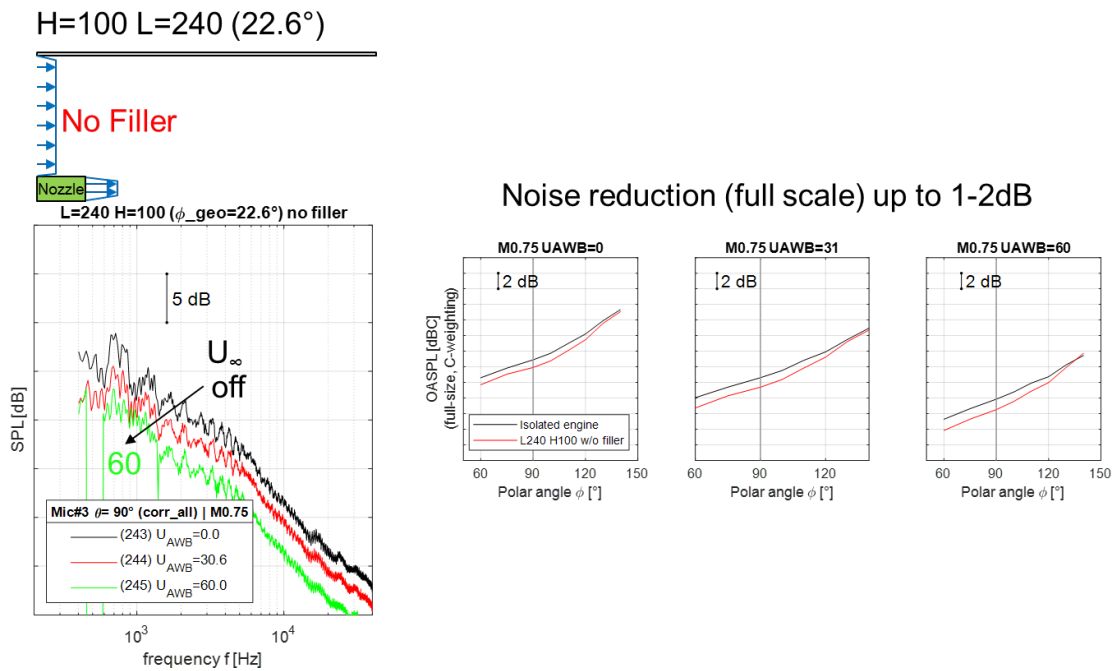


Figure 14: Conventional jet noise shielding on L240 H100 (no filler)

VI. Shielding by direction (over-wing - under-wing)

The difference of mics FF03 (90°, under-plate, GRAS 40BF) and FF13 (−90°, over-plate, B&K 4135) can be used to calculate the shielding between an observer above the plate and underneath the plate. The effect of this type of shielding occurs for all configurations; but as shown before, none of the step configurations and aft-decks examined produces less noise than the isolated jet engine (for static and flight operations). The argumentation is:

$$\text{Isolated jet noise} < \text{installed noise (under-plate)} < \text{installed noise (over-plate)}$$

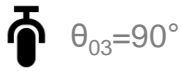
The turbulent flow geometries which is shorter than plate length can be deflected at the plate and thus be shielded from the under-wing observers. The minimal shielding frequency (over-under plate) can be estimated with Helmholtz number $He > 1$:

$$f_s = \frac{He \cdot a_\infty}{L} > \frac{340 \text{ m/s}}{0.240 \text{ m}} = 1.4 \text{ kHz} \quad (4)$$

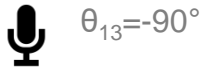
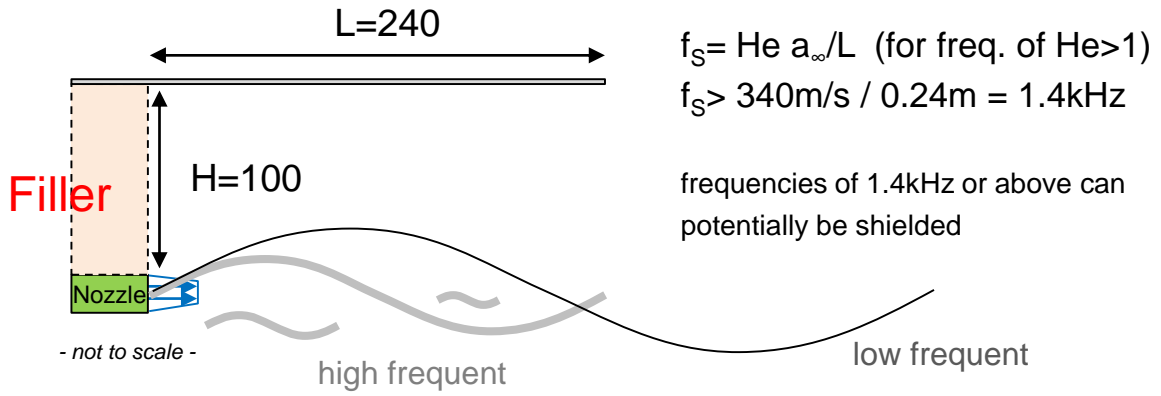
Any lower frequency should not be shielded. A symmetrical test case, i.e. isolated jet noise, can be used to calibrate the corrected data for over-wing and under-wing microphone. There may be a small offset for the symmetrical case which result from differences, e.g. in true mic distance or microphone type. This measured offset can be tabulated for all engine operations (i.e. the combination of jet speed and wind tunnel speed) and used for evaluation. The shielding results with offset calibration look smoother (figure 15, bottom). An impressive high-frequent shielding effect can be measured on the shielded side (1). However, this benefit does not convert into OASPL reduction, one reason being that the installation of the plate comes with a low-frequent penalty (2). The question can be raised whether a short plate above(!) a jet can utilize the deflection effect to allow the jet to turn away from the observer. Could this possibly help to reduce noise?

The experimental data from DLR does not allow us to see the full picture since there is only one installed over-wing microphone (FF13, 90°). However, the experimental data from NASA¹ for $L/H=2.8$ shows that in the rearward arc (i.e. above 105°) this concept works to some extent for the directional shielding: The unshielded side faces $\approx 0.5dB$ less noise than the shielded side. Moreover, it can be argued that there is a small benefit in conventional shielding of isolated jet peak noise to the peak noise on the unshielded side.

GRAS 40BF – under plate



shielded side



BK 4135 – over plate

unshielded side

SHIELDING over-wing - under-wing
L240 H100 w/filler | M0.75 UAWB=0

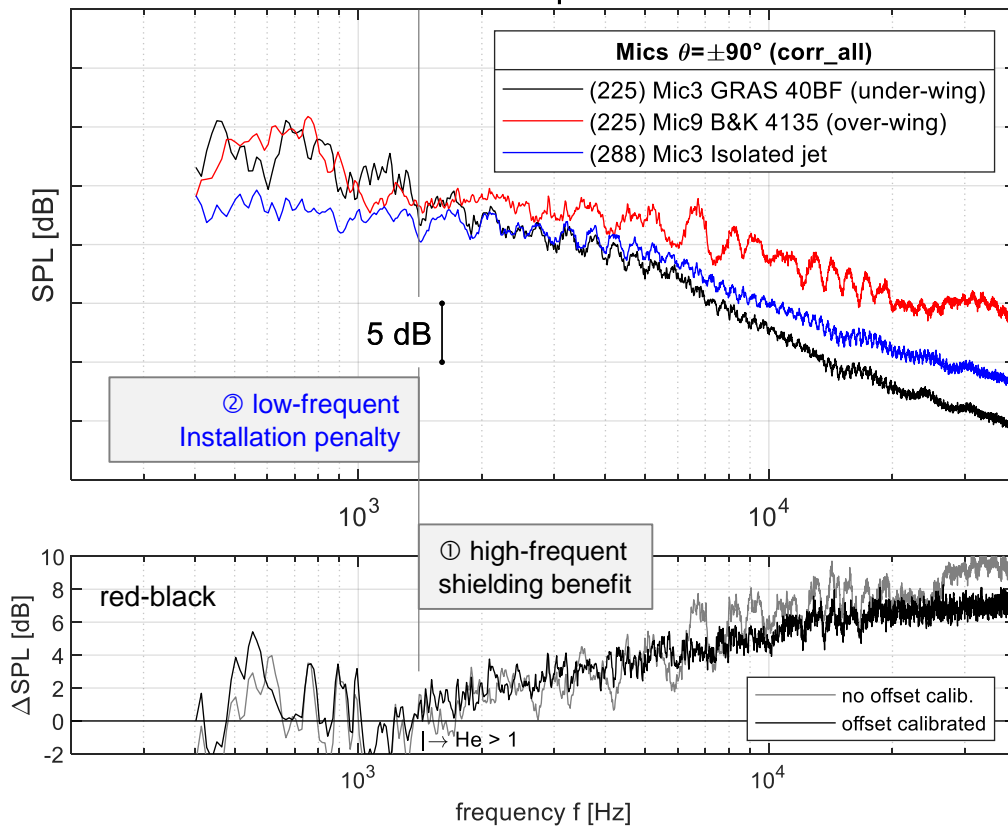


Figure 15: Shielding of noise at under-wing position

VII. Data validity

Massey, Ahuja, & Gaeta³ put a lot of effort into scaling jet noise from rectangular nozzles with different aspect ratio. The results of their scaling efforts indicate that the physics of rectangular jet noise is not as universal as the physics for round circular jet noise.⁴ The reason behind this is likely that the change in aspect-ratio is not self-similar. The efforts of scaling rectangular jet noise of various aspect ratio could be compared with the efforts of scaling high aspect ratio elliptical and circular jets.

However, for the same nozzle (here AR13.3), it can be shown that the velocity scaling works well. The narrowband scaling has to be conducted for $SPL_{nb} - 10 \lg(\Delta f H_0 / U_j)$, whereby the geometric scale H is the same for all spectra (same nozzle), a frequency band is $\Delta f = 12.57 \text{ Hz}$ and U_j is the jet speed. Third-octave spectra scaling can be conducted with $SPL_{1/3} - 10 \lg(f_{sc} H_0 / U_j)$, where the frequency band width is $f_{sc} \approx 0.2316 f_{1/3}$. The static jet noise spectra collapse according to U_j^8 well within a band of $\approx 1 - 2 \text{ dB}$ (see figure 16). The measured data shows especially the high frequent part of the jet noise spectrum whereas the low frequent part is more difficult to detect. Frequencies above 500 Hz or $Sr > 0.05$ are good lower limits for static jet noise. Flight jet noise was examined for self-similar

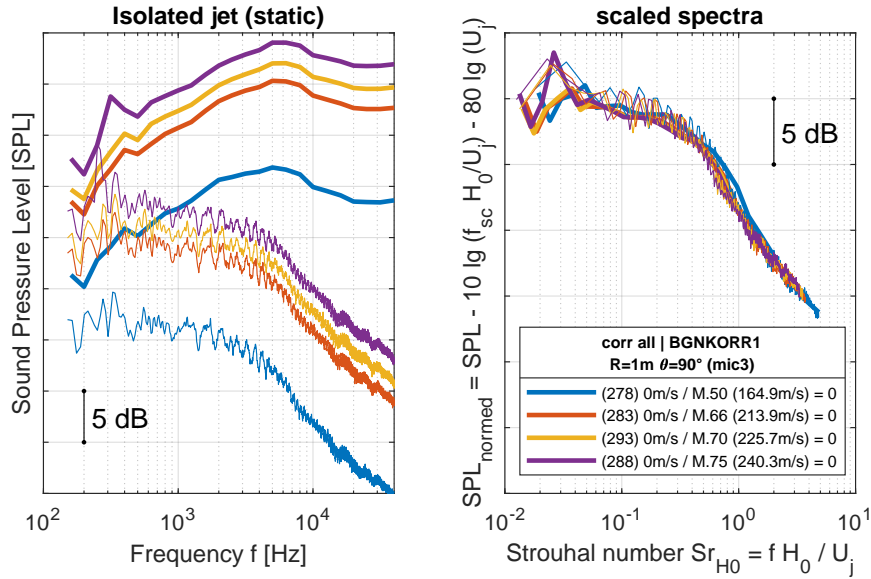


Figure 16: Jet noise scaling for static operations, overhead position

S/L velocity profiles (i.e. const. velocity ratio of $r_U \approx 0.25$). This allows to scale the spectra with any velocity parameter (see figure 17). The spectra scale well with U_j^8 and depict higher frequencies well. Lower frequencies are good above $f \approx 800 \text{ Hz}$. Spectra in the forward arc or at the overhead position looks like pink noise (figure 18).

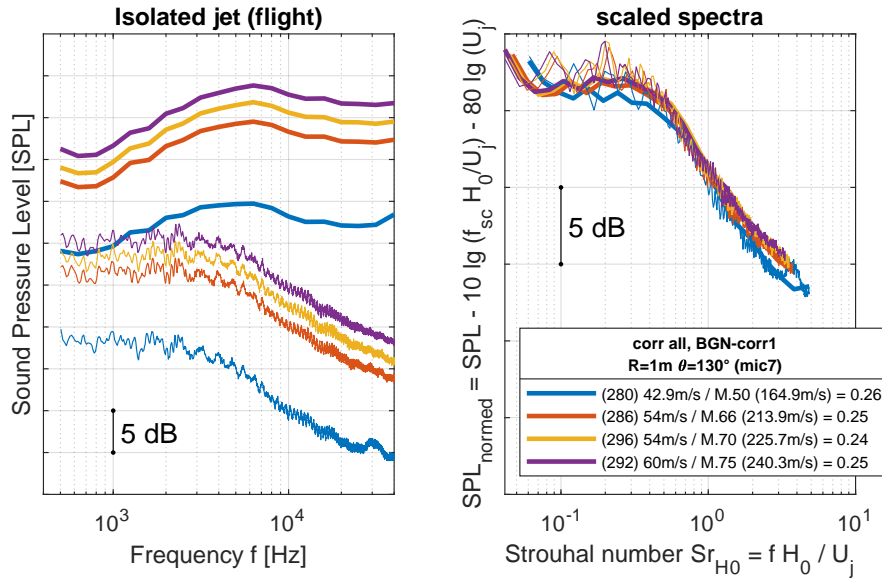


Figure 17: Jet noise scaling for flight operations, rearward arc

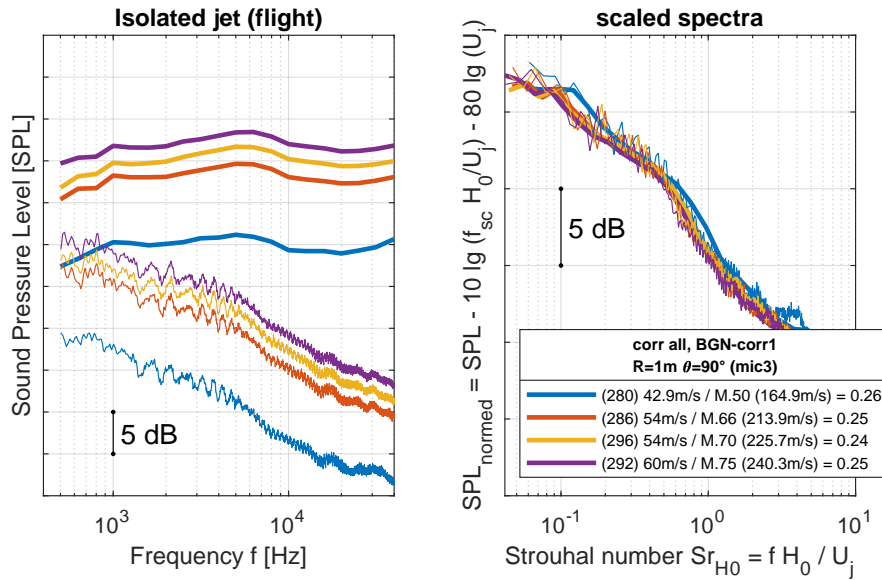


Figure 18: Jet noise scaling for flight operations, overhead position

VIII. Summary and outlook

The tested step-configurations and aft-decks could be structured into the problem physics of an asymmetric nozzle, jet-surface interaction and the wide-angle installation by proposing and using a raw scheme of an aero-geometric model.

The methods to evaluate under-wing vs over-wing shielding (same build, different mic) work and show good results. Noise reduction occurs for high-frequent Helmholtz numbers $He_L > 1$ and corresponds to engine integration length L . Unfortunately, the plate installation causes a low frequent installation penalty. All in all, the tested embedded engine integrations (aft-decks and filled steps) produce greater noise than the isolated engine.

Harvesting the benefits of shielding (same mic, changed build) of a non-embedded propulsion system is possible and was measured to help decrease full scale noise by 1 dBC in OASPL.

Future work could focus on complementing the aero-geometric physical model by characterizing the turning of the flow caused by the plate installation. Noise reduction tests on embedded engine designs could focus on even shorter aft-deck/bevel lengths than NASA's $L/H_0 = 1.4$ bevel.¹

Acknowledgments

The reported work was part of German national research project INTONE (*Minderung von Triebwerksinstallations- und Hochauftriebslärm*) funded by the German Federal Ministry for Economic Affairs and Energy (BMWi). The author thanks all colleagues from Airbus Defense & Space who contributed to this work.

References

¹Bridges, J., “Acoustic Measurements of Rectangular Nozzles with Bevel,” *18th AIAA/CEAS Aeroacoustics Conference (33rd AIAA Aeroacoustics Conference)*, American Institute of Aeronautics and Astronautics, Colorado Springs, Colorado, 2012.

²Behrouzi, P. and McGuirk, J. J., “Underexpanded Jet Development from a Rectangular Nozzle with Aft-Deck,” *AIAA Journal*, Vol. 53, No. 5, 2015, pp. 1287–1298.

³Massey, K., Ahuja, K., and Gaeta, R., “Noise Scaling for Unheated Low Aspect Ratio Rectangular Jets,” *10th AIAA/CEAS Aeroacoustics Conference*, American Institute of Aeronautics and Astronautics, Reston, Virginia, 2004.

⁴Tam, C. K. W. and Auriault, L., “Jet Mixing Noise from Fine-Scale Turbulence,” *AIAA Journal*, Vol. 37, No. 2, 1999, pp. 145–153.